O. Diekmann R. Durrett
K.P. Hadeler P. Maini H.L. Smith

Mathematics Inspired by Biology

Martina Franca, Italy 1997

Editors: V. Capasso, O. Diekmann

Springer

Fondazione C.I.M.E.

Mathematical Models in Morphogenesis

Philip K. Maini
Centre for Mathematical Biology
Mathematical Institute
24-29 St Giles'
Oxford OX1 3LB
England

Contents

Introduction

Spatial and spatio-temporal patterns occur widely in chemistry and biology. In many cases, these patterns seem to be generated spontaneously. The best known oscillatory reaction is the Belousov-Zhabotinsky reaction, in which bromate ions oxidise malonic acid in a reaction catalysed by cerium, which has the states Ce^{3+} and Ce^{4+}. Sustained periodic oscillations are observed in the cerium ions. If, instead, one uses the catalyst Fe^{2+} and Fe^{3+} and phenanthroline, the periodic oscillations are visualised as colour changes between reddish-orange and blue (see, for example, Murray, 1993, Johnson and Scott, 1996 for review). This system can also exhibit a number of different types of wave structures such as propagating fronts, spiral waves, target patterns and toroidal scrolls (Zaikin and Zhabotinskii, 1970, Winfree, 1972, 1974, Müller *et al.*, 1985, Welsh *et al.*, 1983, Zykov, 1987). Such oscillatory and wave-like patterns also arise in physiology and one of the most widely-studied and important areas of wave propagation concerns the electrical activity in the heart (Panfilov and Holden, 1997). These phenomena have motivated a great deal of mathematical modelling and the analysis of the resultant systems (coupled ordinary differential equations and/or partial differential equations) has led to a greater understanding of the underlying mechanisms involved and suggested control strategies in the case of medical applications (see, for example, Goldbeter, 1996).

The development of spatial pattern and form is one of the central issues in embryology. Although genes control pattern formation, genetics does not give us an understanding of the actual mechanisms involved in patterning. Many models of how different processes can conspire to produce pattern have been proposed and analysed. They range from gradient-type models involving a simple source-sink mechanism (Wolpert, 1969); to cellular automata models in which the tissue is discretised and rules are introduced as to how different elements interact with each other (see, for example, Bard, 1981); to more complicated models which incorporate more sophisticated chemistry and biology. In this chapter we shall focus on some models from the latter category which are based on two very different principles of pattern formation. Broadly speaking there are two ways pattern may form: (1) A spatial pattern in some chemical (morphogen) may be set up which in turn determines cell differentiation. Thus the pattern or structure that we observe is due to the underlying pre-pattern in morphogen. (2) A spatial pattern in cell density is set up and cells in high density aggregations then differentiate. Thus the pattern we observe is due directly to the underlying pattern in cell density.

In the next section we consider the most widely studied pre-pattern model, namely,

reaction-diffusion (RD). The model is formulated and analysed using standard linear and nonlinear techniques. As these techniques carry over to the other models in this chapter, they are considered only for the reaction-diffusion model. The properties of the spatial patterns exhibited by the model are presented and some recent results for modified RD models are discussed. Sections 2 and 3 discuss respectively, cell-chemotactic and mechanical models, which are based on (2) above, namely, they hypothesize that patterning occurs due to cell motion. The models are formulated and in Section 2.2 propagating patterns are considered.

Section 4 considers some examples of the application of these models to biology. Specifically, we focus on skeletal patterning in the vertebrate limb, pigmentation patterns in reptiles and avian skin organ formation. The coupling of patterning models is also discussed. Conclusions are presented in Section 5.

1 Reaction-Diffusion Models

1.1 Model Formulation and Linear Analysis

Let $c(\mathbf{x}, t)$ be the concentration of a chemical at position $\mathbf{x} \in \mathbf{R}^3$ and time $t \in [0, \infty)$. Consider an arbitrary volume $V \subset \mathbf{R}^3$. Then
rate of change of chemical in V = − flux + net production i.e.

$$\frac{d}{dt}\int_V c dv = -\int_{\partial V} \mathbf{F}.d\mathbf{S} + \int_V f(c) dv \tag{1.1}$$

where $\mathbf{F}$ is the flux of chemical per unit area and $f(c)$ is net chemical production per unit volume. Using the divergence theorem, (1.1) becomes

$$\int_V \left\{ \frac{\partial c}{\partial t} + \nabla.\mathbf{F} - f(c) \right\} dv = 0. \tag{1.2}$$

As this is true for all arbitrary volumes V, it follows that

$$\frac{\partial c}{\partial t} = -\nabla.\mathbf{F} + f(c). \tag{1.3}$$

We now need an expression for the flux of chemical in terms of chemical concentration. We use Fick's Law, which states that chemical flux is proportional to the concentration gradient, i.e.

$$\mathbf{F} = -D\nabla c \tag{1.4}$$

where D, the diffusion coefficient, is assumed constant (positive). This models flux from high concentrations to low concentrations. Substituting (1.4) into (1.3) we

obtain the reaction-diffusion equation

$$\frac{\partial c}{\partial t} = D\nabla^2 c + f(c). \tag{1.5}$$

There are many ways to derive (1.5). For example, Turing (1952) considered a one-dimensional row of discrete cells with chemical flow between cells, moving from cells with high chemical concentrations to cells with low chemical concentrations. His model was a system of coupled discrete-differential equations and, when averaged over continuous space, gives (1.5). Alternatively, his system could be viewed as a finite difference discretization of (1.5).

Note that in obtaining (1.5) we have assumed that D is constant and that the net production term, f, depends only on c. More generally, D may also be a function of c (density-dependent diffusion) and both D and f may also have spatio-temporal variation.

To complete the model formulation we need to specify initial conditions, $c(\mathbf{x}, 0) = c_0(\mathbf{x})$ and boundary conditions. The latter may typically be written in the form

$$\theta_1(\mathbf{n}.\nabla)c + (1-\theta_1)c = \theta_2 \text{ on } \partial V \tag{1.6}$$

where $\mathbf{n}$ is the outward normal to the surface ∂V of the volume V, and θ_1 and θ_2 are constants. For example, if $\theta_1 = 1$, $\theta_2 = 0$ then we have zero flux (Neumann) conditions. If, on the other hand, we set $\theta_1 = 0$, then we have fixed (Dirichlet) boundary conditions. If the model was to be solved on a ring, then the appropriate boundary condition would be periodic, $c(0) = c(L)$, where L is the circumference of the ring.

For a system of interacting chemicals (1.5) generalises to

$$\frac{\partial \mathbf{u}}{\partial t} = \mathbf{D}\nabla^2\mathbf{u} + \mathbf{f}(\mathbf{u}), \tag{1.7}$$

where $\mathbf{u}$ is a vector of chemical concentrations, $\mathbf{u} = (u_1, u_2, ..., u_n)^T$;
$\mathbf{f} = (f_1(\mathbf{u}), f_2(\mathbf{u}), ..., f_n(\mathbf{u}))^T$ and models chemical interaction; and $\mathbf{D}$ is an $n \times n$ diffusion matrix. In the simplest examples, $\mathbf{D}$ is a diagonal matrix. More generally, $\mathbf{D}$ can have off-diagonal terms to model cross-diffusion.

The classical reaction-diffusion (RD) system which will be analysed in this section is a system of two chemicals, u and v, reacting and diffusing as follows:

$$\frac{\partial u}{\partial t} = D_1\nabla^2 u + f(u,v) \tag{1.8a}$$

$$\frac{\partial v}{\partial t} = D_2\nabla^2 v + g(u,v). \tag{1.8b}$$

We will assume zero flux boundary conditions. The functions f and g are rational functions of u and v (see examples later).

Definition. A uniform steady state of (1.8) is a state $(u,v) = (u_0, v_0)$ where u_0 and v_0 are constants in time and space, satisfying (1.8) and the boundary conditions.

Zero flux boundary conditions are trivially satisfied by any (u_0, v_0), and equations (1.8) are satisfied by

$$f(u_0, v_0) = g(u_0, v_0) = 0.$$

As u and v represent chemical concentrations, we consider only non-negative solutions to these equations.

Definition. Diffusion-driven instability (or Turing instability) occurs when a steady state, stable in the absence of diffusion, goes unstable when diffusion is present.

We now carry out a linear stability analysis to derive the conditions under which a Turing instability can arise.

Let $u = u_0 + \tilde{u}$, $v = v_0 + \tilde{v}$ where $\tilde{u}$ and $\tilde{v}$ are small perturbations from the steady state values u_0, v_0 of u and v respectively.

Substituting into (1.8) and using a Taylor expansion (ignoring quadratic and higher order terms), the equations for $\tilde{u}$ and $\tilde{v}$ become

$$\frac{\partial \tilde{u}}{\partial t} = D_1\nabla^2\tilde{u} + f_u\tilde{u} + f_v\tilde{v} \tag{1.9a}$$

$$\frac{\partial \tilde{v}}{\partial t} = D_2\nabla^2\tilde{v} + g_u\tilde{u} + g_v\tilde{v} \tag{1.9b}$$

with zero flux boundary conditions, where the partial derivatives f_u, f_v, g_u, g_v are evaluated at (u_0, v_0). We look for a separable solution to (1.9) of the form

$$\tilde{u} = ae^{\lambda t}\phi(\mathbf{x}), \quad \tilde{v} = be^{\lambda t}\phi(\mathbf{x}) \tag{1.10}$$

where

$$\nabla^2\phi + k^2\phi = 0 \tag{1.11}$$

and ϕ satisfies the boundary conditions. The property (1.11) reduces the partial differential equation system (1.9) to an ordinary differential equation system and is equivalent to looking for a Fourier series solution.

Substituting (1.10) into (1.9) leads to the pair of simultaneous equations

$$\begin{pmatrix} \lambda + D_1k^2 - f_u & -f_v \\ -g_u & \lambda + D_2k^2 - g_v \end{pmatrix} \begin{pmatrix} a \\ b \end{pmatrix} = \begin{pmatrix} 0 \\ 0 \end{pmatrix} \tag{1.12}$$

which will have non-trivial solutions $(a, b)^T$ if and only if λ satisfies the dispersion relation

$$\lambda^2 - \{f_u + g_v - k^2(D_1 + D_2)\}\lambda + h(k^2) = 0 \tag{1.13}$$

where

$$h(k^2) = D_1 D_2 k^4 - (D_1 g_v + D_2 f_u)k^2 + f_u g_v - f_v g_u. \tag{1.14}$$

The uniform steady state will be linearly stable if Rl $\lambda(k^2) < 0 \; \forall \; k^2 > 0$ and linearly unstable if $\exists \; k^2 > 0$, such that Rl $\lambda(k^2) > 0$. For diffusion-driven instability we require, firstly, that Rl $\lambda(k^2) < 0$ for $k^2 = 0$, that is, the uniform steady state is stable in the absence of diffusion. Hence we require the roots of the quadratic equation

$$\lambda^2(0) - (f_u + g_v)\lambda(0) + f_u g_v - f_v g_u = 0 \tag{1.15}$$

to have negative real part. This occurs iff

$$f_u + g_v < 0 \text{ and } f_u g_v - f_v g_u > 0. \tag{1.16}$$

Secondly, we require there to exist a positive k^2 for which $\lambda(k^2)$ has positive real part. Given (1.16), this can only occur if $h(k^2) < 0$ for some $k^2 > 0$. Hence we require

$$D_1 g_v + D_2 f_u > 0, \tag{1.17}$$

so that $h(k^2)$ has a minimum at a positive value of $k^2 \left(k^2_{\min} = \dfrac{D_1 g_v + D_2 f_u}{2 D_1 D_2} \right)$, and

$$D_1 g_v + D_2 f_u > 2\sqrt{D_1 D_2 (f_u g_v - f_v g_u)} \tag{1.18}$$

so that this minimum is negative.

Therefore, the conditions for diffusion-driven instability are:

(C.1) $f_u + g_v < 0$

(C.2) $f_u g_v - f_v g_u > 0$

(C.3) $D_1 g_v + D_2 f_u > 0$

(C.4) $D_1 g_v + D_2 f_u > 2\sqrt{D_1 D_2 (f_u g_v - f_v g_u)}$

Under these conditions, at the onset of instability, λ is purely real so that the instability is stationary. [If (1.13) has complex conjugate roots with a positive real part, then the instability is oscillatory.]

Remark 1: (C.1) and (C.3) $\Rightarrow D_1 \neq D_2$.

Remark 2: (C.1) and (C.3) imply that f_u and g_v have opposite signs. This observation, together with (C.2), implies that, to an arbitrary relabelling of species, any two-component kinetic mechanism that can lead to diffusion-driven instability must give rise to a Jacobian in kinetic terms at (u_0, v_0) with the following sign structure:

$$K_p \equiv \begin{bmatrix} - & + \\ - & + \end{bmatrix}, \quad K_c \equiv \begin{bmatrix} - & - \\ + & + \end{bmatrix} \tag{1.19}$$

Definition. A kinetic mechanism for which the Jacobian is of type K_p (type K_c) is said to be a pure (cross) activator-inhibitor mechanism at (u_0, v_0). Note that the type of a mechanism may vary with (u_0, v_0).

Remark 3: (C.1)-(C.4) ensure that there exist wavenumbers $k^2 > 0$ such that $\lambda(k^2) > 0$. For the uniform steady state to be unstable, at least one of these wavenumbers must lead to an *admissible* solution. That is, the corresponding function ϕ must satisfy the boundary conditions. Hence (C.1)-(C.4) are necessary but not sufficient conditions for diffusion-driven instability.

Example. Suppose we are on the one-dimensional domain $[0, L]$. Then, for zero flux boundary conditions, the functions ϕ are $\cos \frac{n\pi x}{L}$, that is, the admissible wavenumbers, k, are $k_n = \frac{n\pi}{L}$, $n = 1, 2, 3, \ldots$.

Remark 4: The onset of instability is termed a *bifurcation* point. If instability is to an oscillatory solution it is termed a Hopf bifurcation. Note that a Hopf bifurcation can only occur in (1.8) at $k = 0$, that is, the bifurcation can only yield temporally oscillating solutions when the stationary point of the associated space-independent equations loses its stability (A full statement of the Hopf bifurcation theorem can be found in any standard bifurcation textbook).

Consider now the mechanism K_p. Here $g_u < 0$ so that u *inhibits* v, while $f_v > 0$, so that v *activates* u. Furthermore, condition (C.1) $\Rightarrow |f_u| > |g_v|$, so from (C.3) $D_1 > D_2$. That is, the activator diffuses more slowly than the inhibitor. This is an example of the classic property of many self-organising systems, namely *short-range activation, long-range inhibition.*

In Turing's original model, f and g were linear so that, if the uniform steady state became unstable, then the chemical concentrations would grow exponentially. This, of course, is biologically unrealistic. Since Turing's paper, a number of models have been proposed wherein f and g are nonlinear so that when the uniform steady

state becomes unstable, it may or may not evolve to a bounded, stationary, spatially non-uniform, steady state (a *spatial pattern*) depending on the nonlinear terms.

These models may be classified into four types:

(i) Phenomenological Models: The functions f and g are chosen so that one of the chemicals is an activator, the other an inhibitor. An example is the Gierer-Meinhardt model (1972):

$$\frac{du}{dt} = \underset{\text{source}}{\alpha} - \underset{\substack{\text{linear}\\ \text{degradation}}}{\beta u} + \underset{\substack{\text{autocatalysis in } u/\\ \text{inhibition from } v}}{\frac{\gamma u^2}{v}} \tag{1.20}$$

$$\frac{dv}{dt} = \underset{\substack{\text{activation}\\ \text{by } v}}{\delta u^2} - \underset{\substack{\text{linear}\\ \text{degradation}}}{\eta v}$$

where $\alpha, \beta, \gamma, \delta$ and η are positive constants.

(ii) Hypothetical Models: Derived from a hypothetically proposed series of chemical reactions. For example, Schnakenberg (1979) proposed a series of trimolecular autocatalytic reactions involving two chemicals as follows

$$X \underset{k_2}{\overset{k_1}{\rightleftharpoons}} A, \quad B \xrightarrow{k_3} Y, \quad 2X + Y \xrightarrow{k_4} 3X.$$

Using the Law of Mass Action, which states that the rate of reaction is directly proportional to the product of the active concentrations of the reactants, and denoting the concentrations of X, Y, A and B by u, v, a and b, respectively, we have

$$f(u,v) = k_2 a - k_1 u + k_4 u^2 v, \quad g(u,v) = k_3 b - k_4 u^2 v \tag{1.21}$$

where $k_1, ..., k_4$ are (positive) rate constants. Assuming that there is an abundance of A and B, a and b can be considered to be approximately constant.

(iii) Empirical Models: The kinetics are fitted to experimental data. For example, the Thomas (1975) immobilized-enzyme substrate-inhibition mechanism involves the reaction of uric acid (concentration u) with oxygen (concentration v). Both reactants diffuse from a reservoir maintained at constant concentration u_0 and v_0, respectively, onto a membrane containing the immobilized

enzyme uricase. They react in the presence of the enzyme with empirical rate $\frac{V_m uv}{K_m + u + u^2/K_s}$, so that

$$f(u,v) = \alpha(u_0 - u) - \frac{V_m uv}{K_m + u + u^2/K_s}, \quad g(u,v) = \beta(v_0 - v) - \frac{V_m uv}{K_m + u + u^2/K_s} \tag{1.22}$$

where α, β, V_m, K_m and K_s are positive constants.

(iv) Actual Chemical Reactions: Although Turing predicted, in 1952, the spatial patterning potential of chemical reactions, this phenomenon has only recently been realised in actual chemical reactions. Therefore, it is now possible, in certain cases, to write down detailed reaction schemes and derive, using the Law of Mass Action, the kinetic terms.

The first Turing patterns were observed in the chlorite-iodide-malonic acid starch reaction (CIMA reaction) (Castets *et al.*, 1990, De Kepper *et al.*, 1991). The model proposed by Lengyel and Epstein (1991) stresses three processes: the reaction between malonic acid (MA) and iodine to create iodide, and the reactions between chlorite and iodide and chloride and iodide. These reactions take the form

$$MA + I_2 \rightarrow IMA + I^- + H^+$$
$$ClO_2 + I^- \rightarrow ClO_2^- + \frac{1}{2} I_2$$
$$ClO_2^- + 4I^- + 4H^+ \rightarrow Cl^- + 2I_2 + 2H_2O.$$

The rates of these reactions can be determined experimentally. By making the experimentally realistic assumption that the concentration of malonic acid, chlorine dioxide and iodine are constant, Lengyel and Epstein derived the following model:

$$\frac{\partial u}{\partial t} = k_1 - u - \frac{4uv}{1+u^2} + \nabla^2 u$$
$$\frac{\partial v}{\partial t} = k_2 \left[k_3 \left(u - \frac{uv}{1+u^2} \right) + c\nabla^2 v \right]$$

where u, v are the concentrations of iodide and chlorite, respectively and k_1, k_2, k_3 and c are positive constants.

Murray (1982) calculates and compares the parameter space determined by (C.1)-(C.4) for instability in the Gierer-Meinhardt, Schnakenberg and Thomas models.

Remark 5: A key problem in the verification of Turing structures is the required variation of diffusion coefficients. For a general reaction-diffusion system, the ratio may be changed as follows: consider a standard two-species reaction-diffusion system of the form

$$\begin{aligned}\frac{\partial u}{\partial t} &= f(u,v) + D_1\nabla^2 u,\\ \frac{\partial v}{\partial t} &= g(u,v) + D_2\nabla^2 v,\end{aligned}$$

where u is the activator and v the inhibitor. We make the additional assumption that the activator is involved in a reaction of the form:

$$U + S \underset{r_2}{\overset{r_1}{\rightleftharpoons}} C.$$

Assuming that both S and C are immobile, the RD system is now modified to:

$$\begin{aligned}\frac{\partial u}{\partial t} &= f(u,v) - r_1 us + r_2 c + D_1\nabla^2 u\\ \frac{\partial v}{\partial t} &= g(u,v) + D_2\nabla^2 v\\ \frac{\partial c}{\partial t} &= r_1 us - r_2 c\end{aligned}$$

where s and c are the concentrations of S and C, respectively, and r_1, r_2 are rate constants. If r_1 and r_2 are large, then using singular perturbation theory, c can be approximated in terms of u by $c \equiv ru$, where $r = s_0 r_1/r_2$ and we have assumed that the concentration of S remains close to its initial value, s_0.

On addition of the first and third equations above, we obtain the following equation for the activator:

$$(1+r)\frac{\partial u}{\partial t} = f(u,v) + D_1\nabla^2 u$$

thus when $r \gg 1$ the diffusion of the activator is greatly reduced.

This demonstrates how the formation of an immobile complex can reduce the effective diffusion rate of the activator species. It was this type of approach that was first used by Lengyel and Epstein (1991) to explain how Turing structures develop in the CIMA reaction. In this case, starch forms a stable complex with triiodide ions via the reaction

$$S + I^- + I_2 \rightleftharpoons SI_3^-$$

and the high molecular weight of the complex reduces the rate of diffusion.

Remark 6: A characteristic of Turing patterns is the intrinsic relation between the average diffusion coefficient of the reactants and the wavelength of the pattern. This characteristic differentiates Turing patterns from other patterning phenomena. Turing demonstrated that near the bifurcation from a uniform steady state to Turing patterns, the wavelength of the pattern is predicted to be $\sqrt{2\pi T D}$, where $D = \sqrt{D_1 D_2}$, and D_1, D_2 are the diffusion coefficients. T is the period of the limit cycle when the system is at the onset of Hopf bifurcations (temporally-varying pattern).

Using two types of gel, and varying the concentrations of the gels, it is possible to experimentally test if Turing's rule is obeyed for the CIMA reaction (Ouyang *et al.*, 1995). With the above variations, pattern wavelengths can be measured when D is varied over a factor of three. The corresponding plot of average diffusion coefficient against the experimental wavelength confirms Turing's prediction. Experimental measurement of the period of limit cycles at the onset of Hopf bifurcation is also in good agreement with the theoretical predictions.

1.2 Nondimensionalised system

To reduce the number of parameters in a model, appropriate non-dimensionalisation may be used. For example, in the Schnakenberg model (1.21), set $\mathbf{x}^* = \frac{\mathbf{x}}{L}$, $\tau = \frac{t}{T}$, $u^* = \frac{u}{U}$, $v^* = \frac{v}{V}$. Then (1.21) becomes

$$\frac{\partial u^*}{\partial \tau} = \frac{k_2 T a}{U} - k_1 T u^* + k_4 T U V u^{*2} v^* + \frac{D_1 T}{L^2}\nabla^{*2} u^* \tag{1.23a}$$

$$\frac{\partial v^*}{\partial \tau} = \frac{k_3 T}{V} b - k_4 T U^2 u^{*2} v^* + \frac{D_2 T}{L^2}\nabla^{*2} v^* \tag{1.23b}$$

Choosing $T = \frac{1}{k_1}$, $U = V = \sqrt{\frac{k_1}{k_4}}$, $L = \sqrt{\frac{D_1}{k_1}}$, reduces this system to (dropping * for notational convenience):

$$\frac{\partial u}{\partial \tau} = \alpha - u + u^2 v + \nabla^2 u \tag{1.24a}$$

$$\frac{\partial v}{\partial \tau} = \beta - u^2 v + \delta\nabla^2 v \tag{1.24b}$$

where $\alpha = a\frac{k_2}{k_1}\sqrt{\frac{k_4}{k_1}}$, $\beta = b\frac{k_3}{k_1}\sqrt{\frac{k_4}{k_1}}$ and $\delta = \frac{D_2}{D_1}$. The number of parameters has been reduced from eight to three. Of course, the nondimensionalisation is not unique.

1.3 Properties of Spatial Patterns

Conditions (C.1)-(C.4) determine domains in parameter space wherein diffusion-driven instability is possible. From linear analysis, a number of predictions can be

made on the properties exhibited by spatially patterned solutions to the reaction-diffusion system (1.8):

P.1 Pattern complexity depends on domain size:

Under the conditions (C.1)-(C.4), there exists a range of wavenumbers, k, of possible spatial patterns satisfying

$$k_-^2 < k^2 < k_+^2 \tag{1.25}$$

where k_-^2 and k_+^2 are solutions to Rl $\lambda(k^2) = 0$, and Rl $\lambda(k^2) > 0$ for $k^2 \in (k_-^2, k_+^2)$. The values of $k_\pm^2$ depend on the parameters. On one-dimensional domains with zero flux boundary conditions, or Dirichlet conditions fixed at the spatially uniform steady state, admissible wave numbers are of the form $k = \frac{n\pi}{L}$ where $L =$ domain length. Therefore as L increases, n must increase in order for $\frac{n^2\pi^2}{L^2} \in [k_-^2, k_+^2]$. That is, pattern complexity increases with L. On the two-dimensional domain $[0, L_x] \times [0, L_y]$ with zero flux boundary conditions, the spatial component of the linear solution takes the form

$$\phi_{nm} = \cos\frac{n\pi x}{L_x}\cos\frac{m\pi y}{L_y} \tag{1.26}$$

where n and m are integers (at least one of which is non-zero).

Hence admissible k are now of the form $k_{nm}^2 = \left(\frac{n^2}{L_x^2} + \frac{m^2}{L_y^2}\right)\pi^2$. Therefore, if the domain is long and narrow, i.e. $L_x \gg L_y$, then (1.25) will only be satisfied if $m = 0$, i.e., the pattern depends only on the x coordinate.

P.2 Phase relationship between solutions:

At a primary bifurcation point, from equation (1.12),

$$a = \frac{f_v b}{D_1 k^2 - f_u}. \tag{1.27}$$

Therefore, for a pure activator-inhibitor mechanism sgn $a =$ sgn b, while for a cross activator-inhibitor mechanism sgn $a = -$ sgn b. Hence solutions for the pure (cross) activator-inhibitor mechanism are in (out of) phase, at least in the vicinity of the primary bifurcation point.

1.4 Nonlinear Analysis

All the above results are based on linear theory. As the solution begins to grow, however, nonlinear terms become important and linear theory is no longer valid, i.e. linear theory holds on a short time scale but breaks down on a long time scale. It

is possible to calculate the solution in the vicinity of a primary bifurcation point as follows (for full details see, for example, Fife, 1979, Britton 1986, Grindrod, 1996):

Consider the two species RD system in the one space dimension $[0, \pi]$

$$\frac{\partial \mathbf{u}}{\partial t} = \mathbf{f}(\mathbf{u}) + \mathbf{D}\frac{\partial^2 \mathbf{u}}{\partial x^2} \tag{1.28}$$

with zero flux boundary conditions, where $\mathbf{D} = \begin{bmatrix} 1 & 0 \\ 0 & \delta \end{bmatrix}$. Suppose that δ is the bifurcation parameter with critical value δ_c such that the uniform steady state $\mathbf{u}_0$ loses linear stability for $\delta < \delta_c$. Assume that at this point, $\phi_m = \cos mx$ is the first mode to have positive growth rate in time for some integer m.

Set $\delta = \delta_c - \delta_1\varepsilon$, where $\varepsilon \ll 1$ and δ_1 is a constant, and expand any equilibrium solutions via:

$$\mathbf{u}(x) = \mathbf{u}_0 + \sum_{n=1}^{\infty} \varepsilon^{\xi n}\mathbf{u}_n(x) \tag{1.29}$$

where ξ is a positive constant to be determined, and $\mathbf{u}_n = (u_n, v_n)^t$.

Substituting (1.29) into (1.28) and expanding in Taylor series, we have

$$\begin{aligned}\mathbf{f}(\mathbf{u}) \;=\; & \mathbf{f}(\mathbf{u}_0) + \varepsilon^{\xi} d\mathbf{f}(\mathbf{u}_0).\mathbf{u}_1 + \varepsilon^{2\xi}(d\mathbf{f}(\mathbf{u}_0).\mathbf{u}_2 + \frac{1}{2}u_1^2\mathbf{f}_{uu} + u_1v_1\mathbf{f}_{uv} + \frac{1}{2}v_1^2\mathbf{f}_{vv}) \\ & + \varepsilon^{3\xi}(d\mathbf{f}(\mathbf{u}_0).\mathbf{u}_3 + \frac{1}{2}u_1u_2\mathbf{f}_{uu} + (u_1v_2 + u_2v_1)\mathbf{f}_{uv} + \frac{1}{2}v_1v_2\mathbf{f}_{uv} \\ & + \frac{1}{6}u_1^3\mathbf{f}_{uuu} + \frac{1}{2}u_1^2v_1\mathbf{f}_{uuv} + \frac{1}{2}u_1v_1^2\mathbf{f}_{uvv} + \frac{1}{6}v_1^3\mathbf{f}_{vvv}) \\ & + O(\varepsilon^{4\xi}),\end{aligned}$$

where $d\mathbf{f}(\mathbf{u}_0)$ is the Jacobian of $\mathbf{f}$ evaluated at $\mathbf{u}_0$, and $\mathbf{f}_{uu}, \mathbf{f}_{uv}$ etc. denote the vectors obtained by partially differentiating $\mathbf{f}$ componentwise, evaluated at $\mathbf{u}_0$.

Equating powers of ε we find that $\xi = \frac{1}{2}$. Denoting by L the linear opeartor

$$L\mathbf{u} = \left\{\mathbf{D}\frac{\partial^2}{\partial x^2} + d\mathbf{f}(\mathbf{u}_0)\right\}\mathbf{u}$$

we find that at $O(\varepsilon^{1/2})$,

$$L\mathbf{u}_1 = 0.$$

Thus $\mathbf{u}_1 = A\mathbf{a}\cos mx$ where $\mathbf{a}$ is an eigenvector of the matrix

$$L_m = d\mathbf{f}(\mathbf{u}_0) - m^2\mathbf{D}$$

and A is a real constant to be determined. At $O(\varepsilon)$, $L\mathbf{u}_2 = \mathbf{R}_2$ which can be solved to give $\mathbf{u}_2 = B\mathbf{a}\cos mx + \mathbf{b}\cos 2mx$, where B is some constant and $\mathbf{b}$ can be found in terms of the components of $\mathbf{a}$ and the constant A.

At $O(\epsilon^{3/2})$ we have

$$L\mathbf{u}_3 = \mathbf{R}_3$$

where $\mathbf{R}_3$ contains secular terms. Using the Fredholm Alternative, the solvability condition is that $\mathbf{R}_3$ must be orthogonal to $\mathbf{a}^* \cos mx$ as functions in $L_2((0,\pi), \mathbf{R}^2)$, where $\mathbf{a}^*$ is an eigenvector of the adjoint of L_m. That is,

$$\int_0^\pi \mathbf{R}_3^t . \mathbf{a} \cos mx dx = 0.$$

This leads to an equation of the form

$$0 = A(\delta_1 + lA^2)$$

where the Landau constant l can be found in terms of the parameters of the system (but is independent of the bifurcation parameter δ_1). Hence we have the solution

$$\mathbf{u} = \mathbf{u}_0 \pm \sqrt{\frac{\delta_c - \delta}{\delta_1}} |A_0| \tilde{\mathbf{a}} \cos mx + O(\delta_c - \delta), \tag{1.30}$$

where $A_0^2 = -\delta_1/l$ (if the latter is positive). Thus, $l < 0$ yields the existence of a stable spatially period pattern for $\delta_1 > 0$ (a supercritical bifurcation), while $l > 0$ yields the existence of an unstable spatially periodic pattern for $\delta_1 < 0$ (a subcritical bifurcation). See, for example, Sattinger (1972).

Remark 1. Note that this analysis holds only in the vicinity of a bifurcation point, that is, for ϵ small, and is termed a *weakly nonlinear analysis*. To study solution behaviour far away from the steady state one must use other techniques, for example, numerical continuation and bifurcation techniques. The software package AUTO (Doedel, 1986), for example, discretizes the steady state equations using finite differences and solves the resulting nonlinear algebraic system.

Remark 2. This type of analysis can be carried out on domains of more than one space dimension. In this case, the problem of degeneracy can arise. For example, consider the domain $[0, 2\pi] \times [0, 2\pi]$ with zero flux boundary conditions and assume without loss of generality that the first unstable mode occurs at the wavenumber $k = 1$. Then

$$\mathbf{u}_1 = \mathbf{a}(A_1 \cos x + A_2 \cos y)$$

where A_1 and A_2 are arbitrary constants to be determined. Note that $A_1 = 0$, $A_2 \neq 0$ corresponds to a 'stripe' parallel to the x axis, $A_1 \neq 0$, $A_2 = 0$ corresponds to a 'stripe' parallel to the y axis, while if both A_1 and A_2 are non-zero and in particular, equal,

then we have a 'spot'. Extending the above weakly nonlinear analysis to such a case in two dimensions Ermentrout, 1991, showed that both types of solution could exist but that they were mutually exclusive as stable patterns. Specifically, in a symmetric system with no quadratic terms and only cubic terms, stripes are always selected over spots. Spots can only stably exist if quadratic terms are present in the nonlinearities. However, Benson *et al.*, (1997), have shown that when a spatially varying diffusion is included it is possible to force an RD system that would exhibit stable spots to exhibit stable stripes.

1.5 Inhomogeneous Domains and the Role of boundary conditions

The linear analysis presented in Section 1.1 holds for the case of spatially uniform parameters and zero flux boundary conditions (or Dirichlet conditions, fixed at the spatially uniform steady state). Here we consider two cases where neither of these conditions hold.

(a) Inhomogeneous domain. Let us consider a one-dimensional domain, $x \in [0, 1]$, where the diffusion coefficients of one of the chemicals is spatially non-uniform. For simplicity, let us assume that in the general two chemical RD system we have nondimensionalised the equations such that $D_1 = 1$, and that $D_2 = D(x)$ is the step function

$$D(x) = \begin{cases} D^-, & 0 \leq x < \xi \\ D^+, & \xi < x \leq 1 \end{cases}$$

where $\xi \in (0, 1)$ and $D^- < D^+$.

The requirements for (u_0, v_0) to be stable to spatially homogeneous perturbations remain as before. To derive the analogues of (C.3) and (C.4), we linearise the model about the steady state (u_0, v_0), and look for separable solutions of this linearized system, in the form $u - u_0 = e^{\lambda t} X_u(x)$, $v - v_0 = e^{\lambda t} X_v(x)$. Substituting into the linearized model gives coupled ordinary differential equations for X_u and X_v:

$$X_u'' + (a - \lambda) X_u + b X_v = 0 \tag{1.31a}$$

$$[D(x) X_v']' + c X_u + (d - \lambda) X_v = 0; \tag{1.31b}$$

here prime denotes d/dx and, for notational simplicity, we denote by a, b, c, d, the values of f_u, f_v, g_u, g_v, respectively, at (u_0, v_0). We consider these equations separately

on $[0,\xi)$ and $(\xi,1]$. In the former case, adding (1.31a) to s^-/D^- times (1.31b) gives:

$$(X_u + s^- X_v)'' + \left[a - \lambda + \frac{cs^-}{D^-}\right]\left[X_u + \frac{[b + (d-\lambda)s^-/D^-]}{[a - \lambda + cs^-/D^-]} X_v\right] = 0. \tag{1.32}$$

We choose s^- such that:

$$\frac{b + (d-\lambda)s^-/D^-}{a - \lambda + cs^-/D^-} = s^-. \tag{1.33}$$

which is a quadratic equation for s^-, with roots s_1^- and s_2^- say. Equation (1.32) then becomes a single equation in $X_u + s_j^- X_v$, for $j = 1,2$, with general solution $C_j \cos(\alpha_j^- x) + D_j \sin(\alpha_j^- x)$. Here C_j and D_j are constants of integration, and $\alpha_j^- = [a - \lambda + cs_j^-/D^-]^{1/2}$, $j = 1,2$. We therefore have two simultaneous equations for $X_u(x)$ and $X_v(x)$ in $[0,\xi)$. Solving these and applying zero flux boundary conditions at $x = 0$ gives:

$$X_u(x) = \frac{1}{(s_2^- - s_1^-)}\left[\frac{(\Gamma_u + s_1^-\Gamma_v)s_2^-}{\cos(\xi\alpha_1^-)}\cos(\alpha_1^- x) - \frac{(\Gamma_u + s_2^-\Gamma_v)s_1^-}{\cos(\xi\alpha_2^-)}\cos(\alpha_2^- x)\right] \tag{1.34a}$$

$$X_v(x) = \frac{1}{(s_2^- - s_1^-)}\left[\frac{(\Gamma_u + s_2^-\Gamma_v)}{\cos(\xi\alpha_2^-)}\cos(\alpha_2^- x) - \frac{(\Gamma_u + s_1^-\Gamma_v)}{\cos(\xi\alpha_1^-)}\cos(\alpha_1^- x)\right] \tag{1.34b}$$

on $[0,\xi)$, where $\Gamma_u = X_u(\xi)$, $\Gamma_v = X_v(\xi)$. In (1.34), we are assuming that $s_1^- \neq s_2^-$ and $\cos(\xi\alpha_j^-) \neq 0$ for 1,2; these special cases are discussed in Benson *et al.*, (1993). Similarly, on $(\xi,1]$:

$$X_u(x) = \frac{1}{(s_2^+ - s_1^+)}\left[\frac{(\Gamma_u + s_1^+\Gamma_v)s_2^+}{\cos((1-\xi)\alpha_1^+)}\cos(\alpha_1^+(1-x)) - \frac{(\Gamma_u + s_2^+\Gamma_v)s_1^+}{\cos((1-\xi)\alpha_2^+)}\cos(\alpha_2^+(1-x))\right] \tag{1.34c}$$

$$X_v(x) = \frac{1}{(s_2^+ - s_1^+)}\left[\frac{(\Gamma_u + s_2^+\Gamma_v)}{\cos((1-\xi)\alpha_2^+)}\cos(\alpha_2^+(1-x)) - \frac{(\Gamma_u + s_1^+\Gamma_v)}{\cos((1-\xi)\alpha_1^+)}\cos(\alpha_1^+(1-x))\right]. \tag{1.34d}$$

By design, this solution is continuous at $x = \xi$, but we also require it to satisfy continuity of flux, that is:

$$\lim_{x\to\xi^-} X_u'(x) = \lim_{x\to\xi^+} X_u'(x) \quad \lim_{x\to\xi^-} D^- X_u'(x) = \lim_{x\to\xi^+} D^+ X_v'(x). \tag{1.35}$$

Substituting the solutions (1.34) into (1.35) gives:

$$P(\lambda)\Gamma_u + Q(\lambda)\Gamma_v = 0$$

$$R(\lambda)\Gamma_u + S(\lambda)\Gamma_v = 0,$$

where

$$\begin{aligned}
P(\lambda) &= (s_1^- T_2^- - s_2^- T_1^-)/(s_2^- - s_1^-) + (s_1^+ T_2^+ - s_2^+ T_1^+)/(s_2^+ - s_1^+) \\
Q(\lambda) &= s_1^- s_2^-(T_2^- - T_1^-)/(s_2^- - s_1^-) + s_1^+ s_2^+(T_2^+ - T_1^+)/(s_2^+ - s_1^+) \\
R(\lambda) &= D^-(T_1^- - T_2^-)/(s_2^- - s_1^-) + D^+(T_1^+ - T_2^+)/(s_2^+ - s_1^+) \\
S(\lambda) &= D^-(s_1^- T_1^- - s_2^- T_2^-)/(s_2^- - s_1^-) + D^+(s_1^+ T_1^+ - s_2^+ T_2^+)/(s_2^+ - s_1^+)
\end{aligned}$$

and $T_j^- = \alpha_j^- \tan(\xi\alpha_j^-)$, $T_j^+ = \alpha_j^+ \tan((1-\xi)\alpha_j^+)$, for $j = 1,2$. Now from (1.34), $\Gamma_u = \Gamma_v = 0$ implies that $X_u(x) \equiv X_v(x) \equiv 0$. Thus for non-trivial X_u and X_v, we require:

$$F(\lambda) \equiv P(\lambda)S(\lambda) - Q(\lambda)R(\lambda) = 0. \tag{1.36}$$

This is the dispersion relation, relating growth rates of instabilities to the model parameter values. The model system will exhibit diffusion-driven instability provided (C.1) and (C.2) are satisfied, and provided this dispersion relation has a solution with positive real part. Our derivation of (1.34) assumes that $\cos(\xi\alpha_1^-)$, $\cos(\xi\alpha_2^-)$, $\cos((1-\xi)\alpha_1^+)$, $\cos((1-\xi)\alpha_2^+)$ and $(s_1^+ - s_2^+)$ are all non-zero. Similar analysis can be done in the cases when one or more of these is zero, but the solutions for u and v cannot in general satisfy continuity of flux at $x = \xi$. One notable exception to this, however, is the homogeneous case $D^- = D^+$. The solutions of the dispersion relation given by the standard analysis (see above) satisfy $\alpha_j^\pm = n\pi$ for some $n \in [1,2,3,\ldots\}$ and either $j = 1$ or $j = 2$. Thus with $\xi = 1/2$, half of the eigenvalues λ are not roots of (1.33), since $\cos(n\pi/2) = 0$ when n is even. These roots can be retrieved, however, either by investigating the above special cases, or by taking more general values of ξ: the value of ξ is irrelevant when $D^- = D^+$.

A typical functional form of $F(\lambda)$ is illustrated in Fig. 1.1 (see Maini *et al.*, 1992 and Benson *et al.*, 1993 for full details).

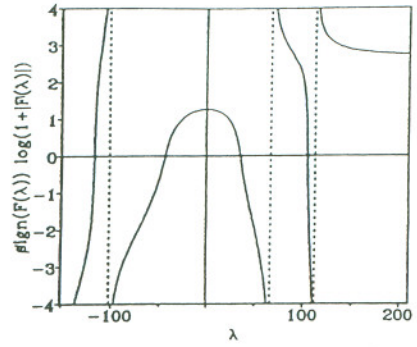

Figure 1.1: A typical functional form of the dispersion relation $F(\lambda)$ defined in (1.36) for Schnakenberg kinetics. (See Maini *et al.*, 1992, Figure 2, for full details). Reproduced from Maini *et al.*, 1992, by permission of Oxford University Press.

(b) Mixed boundary conditions. For boundary conditions of the form (1.6), a uniform steady state will not, in general, exist and therefore the linear analysis of Section 1.1 cannot be carried out. Here we consider a special case where a uniform steady state does exist but each chemical satisfies a different boundary condition. Consider the one-dimensional domain [0,1] and suppose that u is fixed at u_0 on the boundary, while v satisfies zero flux boundary conditions. The linearised system (1.9) now has solutions of the form

$$\begin{pmatrix} \tilde{u} \\ \tilde{v} \end{pmatrix} = e^{\lambda t}\Phi(x)$$

where

$$\Phi = \begin{pmatrix} \sum_{m=1}^{\infty} A_m \sin(m\pi x) \\ \sum_{n=0}^{\infty} B_n \cos(n\pi x) \end{pmatrix}. \tag{1.37}$$

By contrast, in the classical linear problem with scalar homogeneous Neumann conditions, the n^{th} eigenfunction is of the form

$$\Phi = \begin{pmatrix} A_n \\ B_n \end{pmatrix} \cos(n\pi x). \tag{1.38}$$

Substituting (1.37) into the linearised system we obtain

$$\sum_{m=1}^{\infty}[\lambda + v(m\pi)^2 - a]A_m \sin(m\pi x) = \sum_{n=0}^{\infty} bB_n \cos(n\pi x)$$

$$\sum_{n=0}^{\infty}[\lambda + v\delta(n\pi)^2 - d]B_n \cos(n\pi x) = \sum_{m=1}^{\infty} cA_m \sin(m\pi x). \tag{1.39}$$

Multiplying through by $\sin(m\pi x)$ and integrating over [0,1] leads to

$$\begin{aligned} [\lambda + v(m\pi)^2 - a]A_m &= \sum_{n=0}^{\infty} bB_n\alpha_{nm} \\ cA_m &= \sum_{n=0}^{\infty}[\lambda + v\delta(n\pi)^2 - d]B_n\alpha_{nm} \end{aligned} \tag{1.40}$$

where

$$\alpha_{nm} = \frac{\langle \cos(n\pi x), \sin(m\pi x)\rangle}{\langle \sin(m\pi x), \sin(m\pi x)\rangle} \text{ and } \langle f, g\rangle = \int_0^1 f(x)g(x)dx.$$

System (1.40) is an infinite system of linear equations for the infinite number of unknowns A_m, B_n, $m = 1, 2, 3, ..., n = 0, 1, 2, 3, ...$ To solve this system we make a finite dimensional approximation (FDA) by considering only values of m up to M and truncating the sums at $n = M - 1$. This leads to a system of $2M$ equations for the $2M$ unknowns $(A_1, A_2, ..., A_M, B_0, B_1, ..., B_{M-1})$. We may rewrite the truncated system as the generalized eigenvalue problem

$$\mathbf{P}\mathbf{x} = \lambda\mathbf{Q}\mathbf{x} \tag{1.41}$$

where $\mathbf{x} = (A_1, A_2, ..., A_M, B_1, ..., B_{M-1})$ and $\mathbf{P}$ and $\mathbf{Q}$ are $2M \times 2M$ matrices which have the block structure

$$\mathbf{P} \equiv \begin{bmatrix} \mathbf{P}_1 & \mathbf{P}_2 \\ \mathbf{P}_3 & \mathbf{P}_4 \end{bmatrix}, \quad \mathbf{Q} \equiv \begin{bmatrix} -\mathbf{I} & \mathbf{0} \\ \mathbf{0} & \mathbf{Q}_4 \end{bmatrix}.$$

Here $\mathbf{P}_i$ and $\mathbf{Q}_i$ are $M \times M$ matrices given by

$$\begin{aligned} (\mathbf{P}_1)_{ij} &= \begin{cases} 0 & \text{if } i \neq j \\ v(m\pi)^2 - a & \text{if } i = j \end{cases} \\ (\mathbf{P}_2)_{ij} &= -b\alpha_{j-1,i} \quad \mathbf{P}_3 = c\mathbf{I} \\ (\mathbf{P}_4)_{ij} &= (v\delta(j-1)^2\pi^2 - d)\alpha_{j-1,i} \\ (\mathbf{Q}_4)_{ij} &= \alpha_{j-1,i} \end{aligned}$$

where $i, j = 1, 2, ..., M$, and $\mathbf{I}$ is the $M \times M$ unit matrix.

The solution of (1.41) leads to $2M$ eigenvalues λ_i with corresponding eigenvectors $\mathbf{x}_i$. Thus the M-dimensional approximation to the solution is

$$\begin{pmatrix} \tilde{u}_1 \\ \tilde{v}_2 \end{pmatrix} = \sum_{i=1}^{2M} \begin{pmatrix} \sum_{m=1}^{M} A_{mi} \sin(m\pi x) \\ \sum_{n=0}^{M-1} B_n \cos(n\pi x) \end{pmatrix} e^{\lambda_i \tau} \tag{1.42}$$

where $(A_{1i}, A_{2i}, ..., A_{Mi}, B_{0i}, B_{1i}, ..., B_{(M-1)i})$ is the eigenvector with eigenvalue λ_i.

As the dimension of the FDA is increased, the values of the previously calculated eigenvalues and eigenvectors will change and more eigenvalues and corresponding eigenvectors will be generated. We use the following criteria as stopping tests.

(i) The approximation for a chosen λ_i and its corresponding eigenvector must converge as the dimension of the FDA is increased. In the case of the eigenvectors this also means that higher order terms are insignificant. For any given λ_i there is an M_c such that the computed eigenvalue and eigenvector are sufficiently accurate for $M = M_c$.

(ii) The eigenvalues introduced for $M > M_c$ have real part negative, and thus correspond to temporally decaying solutions of the linearised system.

If both these criteria are satisfied, then we are assured that the FDA only ignores exponentially decaying terms in time and insignificantly small terms in the trigonometric expansion of the spatial component of the solution to the linearised problem. Furthermore, if some of the eigenvalues obtained by the FDA have positive real part, then the uniform steady state is unstable and we postulate that the solution will evolve to a spatially varying solution of the form (1.42) with temporal growth rates given by the real part of the positive eigenvalues (assuming, of course, that a bounded solution exists). This procedure is illustrated in Dillon *et al.*, (1994).

We can gain some insight into the connection with the Neumann problem as follows. Note that the system (1.40) may be reduced by eliminating A_m to

$$\sum_{n=0}^{\infty}[(\lambda + v(m\pi)^2 - a)(\lambda + v\delta(n\pi)^2 - d) - bc]\alpha_{nm}B_n = 0 \qquad (1.43)$$

for $m = 1, 2, 3, ...$

This may be written as

$$\sum_{n=0}^{\infty}\{\lambda^2 + [v(m\pi)^2 + \delta v(n\pi)^2 - \text{ trace } K]\lambda + \delta v^2(m\pi)^2(n\pi)^2 - [av(m\pi)^2 + dv(n\pi)^2] + \text{ det } K\}B_n\alpha_{nm} = 0,$$

where K is the Jacobian matrix $\begin{bmatrix} a & b \\ c & d \end{bmatrix}$.

As $\alpha_{nm} = 0$ for $n + m = 2p$, the infinite system represented by (1.43) can be written as

$$\Omega(\lambda)\mathbf{B} = \begin{bmatrix} \Omega_1(\lambda) & 0 \\ 0 & \Omega_2(\lambda) \end{bmatrix}\begin{bmatrix} \mathbf{B}_e \\ \mathbf{B}_o \end{bmatrix}.$$

Here $\mathbf{B}_e = (B_0, B_2 \ldots)^T$ and $\mathbf{B}_o = (B_1, B_3 \ldots)^T$. Thus det $\Omega(\lambda) =$ det $\Omega_1(\lambda)$ det $\Omega_2(\lambda)$ and the eigenvectors decompose into those with only $B_j \neq 0$ for j even and those with only $B_j \neq 0$ for j odd.

The above analysis can be used to locate bifurcation points as a certain parameter p is varied using the method of bisection as follows: we choose a low dimensional FDA, a value of the parameter p, say p_1, at which all eigenvalues have real part negative and another value p_2 at which at least one eigenvalue has positive real part. Assume, without loss of generality, that $p_2 > p_1$. Clearly, a certain number of eigenvalues must cross the axis in (p_1, p_2). By examining the signs of the eigenvalues at the midpoint $(p_1 + p_2)/2$ of the interval we can easily determine in which half of the interval the bifurcation point lies. We can continue this procedure to find the bifurcation point to the required degree of accuracy. By going to a higher dimensional FDA we may obtain a more accurate value of the parameter at the bifurcation point.

2 Cell-Chemotactic Models

2.1 Model Formulation

The model involves two dependent variables, cell density, $n(\mathbf{x}, t)$, and chemoattractant concentration, $c(\mathbf{x}, t)$, where $\mathbf{x}$ and t are the spatial coordinate and time, respectively. Following Section 1.1, these variables satisfy the equations

$$\frac{\partial n}{\partial t} = -\nabla.\mathbf{J}_n + f(n, c) \qquad (2.1)$$

$$\frac{\partial c}{\partial t} = -\nabla.\mathbf{J}_c + g(n, c) \qquad (2.2)$$

where $\mathbf{J}_n, \mathbf{J}_c$ and $f(n, c), g(n, c)$ are cell, chemical flux and net production, respectively. It is assumed that two processes contribute to cell flux: random motion, and motion in response to gradients in chemical concentration. Hence

$$\mathbf{J}_n = \mathbf{J}_n^d + \mathbf{J}_n^c \qquad (2.3)$$

where $\mathbf{J}_n^d = -D_n\nabla n$, that is, Fickian type motion with diffusion coefficient $D_n(> 0)$, and $\mathbf{J}_n^c = \chi(c)n\nabla c$, modelling chemotactic motion. The function $\chi(c)$ measures chemotactic sensitivity and can take a number of forms. For example, the simplest form for $\chi(c)$ is a constant. This assumes that the sensitivity of cells to attractant is independent of attractant concentration. If cell sensitivity to c is known to decrease with c, then one possible form for $\chi(c)$ is α/c where α is a constant (Keller and Segel,

1971). The action of cell surface receptors has been modelled by setting $\chi(c) = \frac{\alpha}{(\alpha_1+c)^2}$ where α and α_1 are constants (Lapidus and Schiller, 1976; Ford and Lauffenberger, 1991). This modelling approach is phenomenological. Recently, Othmer and Stevens (1997) have derived macroscopic chemotaxis equations based on microscopic rules using a random walk approach. They show how specific assumptions at a microscopic level can give rise to the types of phenomenological macroscopic models mentioned above.

Typically, net cell production is assumed to follow logistic growth, that is, $f(n,c) = rn(N-n)$ where r and N are non-negative constants. Hence, at low cell densities, growth is exponential, while at high cell densities (approaching N), cell growth tends to zero.

The chemical is assumed to diffuse according to Fick's Law, hence $\mathbf{J}_c = -D_c\nabla c$, where D_c is the (non-negative) diffusion coefficient. Net chemical production is composed of two parts: production by the cells minus degradation. There are a number of ways to model these terms depending on the biological situation. As an example, chemical production may be a saturating function of cell density, modelled by the term $\frac{Sn}{\beta+n}$, where S and β are positive constants. Here, chemical production rate per unit cell $\frac{S}{\beta+n}$, decreases with cell density, to account for the process of contact inhibition whereby at high cell densities various metabolic pathways are turned off. Degradation may be simply of the form $-\gamma c$, where γ is the rate of linear degradation.

The system (2.1)-(2.2) may be analysed in an analogous fashion to that of (1.8) and shown to have the ability to produce spatial pattern. In this case, activation is due to cells producing chemical which attracts more cells by chemoattraction, while inhibition is due to cell depletion in the neighbourhood of a cell aggregation. However, the nonlinear flux term means that the model is not as well behaved as the standard RD system and cell-chemotactic models can exhibit blow-up (see, for example, Childress and Percus, 1981 and Othmer and Stevens, 1997). A detailed numerical bifurcation analysis of a version of (2.1)-(2.2) in two spatial dimensions was carried out by Maini *et al.*, (1991). Their results are considered in Section 4.3. The model can also exhibit propagating patterns and these will be the focus of study in the next section.

2.2 Propagating Patterns

We consider here the non-dimensionalised version of (2.1)-(2.2) studied, in one spatial dimension, by Myerscough and Murray, 1992:

$$\frac{\partial n}{\partial t} = D_n\frac{\partial^2 n}{\partial x^2} - \alpha\frac{\partial}{\partial x}\left(n\frac{\partial c}{\partial x}\right) \tag{2.4a}$$

$$\frac{\partial c}{\partial t} = \frac{\partial^2 c}{\partial x^2} + \frac{n}{1+n} - c \tag{2.4b}$$

Here, it has been assumed that the chemotactic sensitivity is constant (α) and that, on the timescale of interest, there is no net change in cell density.

Equations (2.4) have a one parameter family of homogeneous steady states

$$n = n_0, \quad c = c_0 = \frac{n_0}{1+n_0} \tag{2.5}$$

where n_0, the average cell density, is a constant parameter. If we assume zero flux boundary conditions, then the initial cell density determines n_0, which can then be considered as a fixed parameter. Linearising (2.4) about (2.5), and solving the resulting equations gives the dispersion relation

$$\lambda^2 + [k^2(D_n+1)+1]\lambda + k^2\left[D_n(k^2+1) - \frac{\alpha n_0}{(1+n_0)^2}\right] = 0. \tag{2.6}$$

Note that in this case $\lambda = 0$ at $k = 0$, so the standard weakly nonlinear theory presented in the previous section does not automatically apply (see Grindrod *et al.*, 1989).

If the system is set initially to a spatially uniform steady state and then a perturbation in cell density is imposed at one end, a regular pattern of standing peaks and troughs is generated progressively. The wavelength of the pattern and its speed of spread appear constant. Myerscough and Murray analysed this propagating pattern with a method based on that developed by Dee and Langer (1983). At the leading edge of the pattern, the amplitude of the disturbance is small and linear theory applies. Therefore, the solution to (2.4) at the leading edge may be written as the integral of Fourier modes

$$n(x,t) = \int_{-\infty}^{\infty} A(k)\exp[ikx + \lambda(k^2)t]dk \tag{2.7}$$

where $\lambda(k^2)$ is given by (2.6) and $A(k)$ is determined by the initial conditions.

This solution is valid at the leading edge and, assuming that the speed of propagation is v, a constant, we have

$$n(vt,t) = \int_{-\infty}^{\infty} A(k)\exp[tg(k)]dk \tag{2.8}$$

where $g(k) = ikv + \lambda(k^2)$. Using the method of steepest descents (see, for example, Murray, 1984), this integral can be evaluated asymptotically for large t and x to yield

$$n \sim \frac{F(k^*)}{\sqrt{t}} \exp[t(ik^*v + \lambda(k^{*2})] \tag{2.9}$$

where F is a function of k which is not important for this particular analysis and k^* is a saddle point of $g(k)$ in the complex k-plane (i.e. a solution to $\frac{dg}{dk} = 0$), chosen so that $\mathrm{Re}(ik^*v + \lambda(k^{*2})) > \mathrm{Re}(ikv + \lambda(k^2))|_{k\in\alpha}$ where α is the set of all saddle points other than k^*.

As the envelope of the pattern is constant in shape far from the initial perturbation, it is assumed that $\mathrm{Re}(g(k^*)) = 0$. This is called the marginal stability hypothesis. Hence, v and k^* satisfy the equations:

$$iv + \frac{d\lambda}{dk} = 0 \tag{2.10}$$

and

$$\mathrm{Re}(ik^*v + \lambda(k^{*2})) = 0. \tag{2.11}$$

Now consider the pattern in the moving frame of the envelope. In this frame, we see an oscillating pattern at the leading edge with frequency of oscillation

$$\Omega = \mathrm{Im}(g(k)). \tag{2.12}$$

This is the frequency at which nodes are created at the front of the envelope. Assuming that peaks do not coalesce and are conserved, this is also the frequency of oscillation far from the leading edge. If k' is the wave number of the pattern far behind the leading edge, then $\Omega = k'v$, so

$$k' = Re(k^*) + Im\frac{\lambda(k^{*2})}{v}. \tag{2.13}$$

This method assumes that the equations are weakly nonlinear in the vicinity of the leading edge and that the behaviour of the solution is determined by the leading edge.

Myerscough and Murray carried out a comparison of the analytical results with numerical simulations and found that for small amplitude solutions there was good quantitative agreement but for large amplitude solutions the agreement was only qualitative. In the latter, nonlinear effects play a crucial role. For example, peaks produced near the leading edge tend to grow and coalesce, hence invalidating the peak counting argument.

An application of the type of propagating patterns discussed in this section is presented in Section 4.3.

3 Mechanical Models

3.1 Model Formulation

The mechanical model proposed by Oster *et al.*, (1983) has three dependent variables: $n(\mathbf{x},t)$, $\rho(\mathbf{x},t)$ and $\mathbf{u}(\mathbf{x},t)$ which represent, respectively, cell density, matrix density and matrix displacement at position $\mathbf{x}$ and time t. The cell and matrix equations take the general form (1.3) and we consider them first.

The cell equation is

$$\frac{\partial n}{\partial t} = -\nabla.\mathbf{J} + rn(N-n) \tag{3.1}$$

where $\mathbf{J}$ is cell flux and cell growth is assumed to be of logistic form. In this case, cell flux is due to three processes.

(i) Random motion, modelled as usual by $\mathbf{J}_d = -D\nabla n$

(ii) Haptotaxis: Cells move by attaching cell processes to adhesive sites within the matrix and crawling along. As cells exert forces on the extracellular matrix (ECM) they generate adhesive gradients which serve as guidance cues to motion. The movement up such gradients is termed haptotaxis. Assuming that the number of adhesive sites is proportional to ECM density, we have that $\mathbf{J}_h = \alpha n\nabla\rho$, where α is the haptotactic coefficient, assumed to be a non-negative constant.

(iii) Advection: As the matrix is deformed, cells may be carried or dragged passively along. This is termed advection and contributes a flux $\mathbf{J}_a = n\frac{\partial \mathbf{u}}{\partial t}$, where $\mathbf{u}$ is the displacement of a material point of ECM.

Hence, the total cell flux, $\mathbf{J}$, is given by $\mathbf{J} = \mathbf{J}_d + \mathbf{J}_h + \mathbf{J}_a$, so that the equation for cell motion is

$$\frac{\partial n}{\partial t} = D\nabla^2 n - \alpha\nabla.(n\nabla\rho) - \nabla.\left(n\frac{\partial \mathbf{u}}{\partial t}\right) + rn(N-n) \tag{3.2}$$

The matrix equation is much simpler as the only contribution to matrix flux is advection, and matrix secretion is assumed negligible. Hence, ρ satisfies

$$\frac{\partial \rho}{\partial t} = -\nabla.\left(\rho\frac{\partial \mathbf{u}}{\partial t}\right) \tag{3.3}$$

To derive the equation for the matrix displacement, $\mathbf{u}(\mathbf{x},t)$, we first note that for cellular and embryonic processes, inertial terms are negligible in comparison to viscous

and elastic forces, that is, motion ceases instantly when the applied forces are turned off. Hence the traction forces generated by the cells are balanced by the viscoelastic forces within the ECM. Therefore the equilibrium equations are

$$\nabla.\sigma + \rho\mathbf{F} = \mathbf{0} \tag{3.4}$$

where σ is the composite stress tensor of the cell-ECM milieu and $\rho\mathbf{F}$ accounts for body forces.

Oster *et al.*, (1983) model the cell-matrix composite as a viscoelastic material with stress tensor

$$\sigma = \sigma_p + \sigma_n. \tag{3.5}$$

Here σ_p is the usual viscoelastic stress tensor (see, for example, Landau and Lifshitz, 1970),

$$\sigma_p = \underbrace{\mu_1\frac{\partial\varepsilon}{\partial t} + \mu_2\frac{\partial\theta}{\partial t}\mathbf{I}}_{\text{viscous}} + \underbrace{\frac{E}{1+\nu}\left(\varepsilon + \frac{\nu}{1-2\nu}\theta\mathbf{I}\right)}_{\text{elastic}} \tag{3.6}$$

where: $\theta = \nabla.\mathbf{u}$ is the dilatation, $\varepsilon = \frac{1}{2}[\nabla\mathbf{u} + \nabla\mathbf{u}^T]$ is the stress tensor, $\mathbf{I}$ is the unit tensor, μ_1, μ_2 are the shear and bulk viscosities, respectively, and E, ν are the Young's modulus and the Poisson ratio, respectively.

The stress due to cell traction is modelled by

$$\sigma_n = \frac{\tau n\rho}{1+\lambda n}\mathbf{I} \tag{3.7}$$

where τ and λ are positive constants. This satisfies the conditions that there is no traction without matrix and that traction per cell decreases with increasing cell density (contact inhibition).

If the cell-matrix composite is attached to an external substatum, for example a subdermal basement layer, then the body force will be

$$\mathbf{F} = s\mathbf{u} \tag{3.8}$$

where s is the modulus of elasticity of the substrate to which the composite is attached.

With appropriate boundary conditions [for example zero flux on n and p, with $\mathbf{u}$ fixed], (3.1)-(3.8) define a simple version of the more complicated mechanical model presented by Oster *et al.*, (1983). The model equations can be analysed in much the same way as the RD system discussed in Section 1 but due to its complexity it is less amenable to analysis and further simplifying assumptions need to be made.

Linear and nonlinear analyses, plus numerical simulation, show that models within this general mechanical framework can exhibit steady-state spatial patterns (Perelson *et al.*, 1986) and spatio-temporal patterns (Ngwa and Maini, 1995).

4 Biological Applications

4.1 Developmental Constraints

Although the models discussed in Sections 1-3 are based on very different biological hypotheses, they share many common mathematical features. In particular, in the vicinity of primary bifurcation points from the uniform steady states, linear analysis predicts spatial patterns that are eigenfunctions of the Laplacian operator with the appropriate boundary conditions. Moreover, the mechanism of "short-range activation, long-range inhibition" that leads to patterning in RD systems may be generalised to the cell-chemotaxis (CC) and mechanical models discussed in Sections 2 and 3. In the CC model, short-range activation is due to chemoattractant secretion by cells increasing with cell density resulting in chemical gradients attracting cells to centres of high cell density. In turn, this creates zones of recruitment separated by regions of virtually zero cell density which inhibit these zones from growing even further. In the mechanical models, short-range activation is due to cell traction dragging cells to areas of high cell density while the long-range inhibition is due to the elastic restoring forces of the external tethering and the paucity of cells in surrounding regions.

Therefore, taking into account these mechanistic and mathematical similarities, it is not surprising that these models exhibit many similarities in their patterning properties. In other words, many of these properties are mechanism independent and are therefore developmental constraints that patterns must satisfy, regardless of their origin (Oster *et al.*, 1988).

We now illustrate the application of the above models to three very different types of biological pattern formation. In light of the above discussion it should be noted that more than one model could account for each of these patterning processes.

4.2 Skeletal patterning in the vertebrate limb

The formation of skeletal patterning in the vertebrate limb has been the focus of a great deal of experimental and theoretical research (for a review, see Maini and Solursh, 1991). Recently, it has been shown that a number of Hox genes are switched on in a precise spatio-temporal manner in the developing chick limb. Although these are exciting advances, they still beg the question of how this patterning of activity is initiated. RD theory, as a model for the generation of such robust processes as digit formation, has been heavily criticised. For example, Bard and Lauder (1974) showed that the qualitative form of the model solutions could be greatly influenced by minor

perturbations in the system such as a small change in length. In such an application, an essential requirement for a model is that it must be able to produce a limited number of patterns in a very robust way. In this respect, the models discussed in this chapter are almost too sophisticated because they exhibit a vast variety of patterns, many of which are never observed. Hence, one is forced to turn the question of pattern formation on its head and ask, how can one *not* generate so much pattern? One way to address this issue is to investigate the role of boundary conditions. The key point here is that certain types of boundary conditions preclude many patterns from forming while extending the domains of stability of the remaining patterns. This has been shown for an RD system in one dimension (Dillon *et al.*, 1994). Figure 4.1 shows a comparison of the patterns formed under zero flux boundary conditions with conditions in which the boundary is a sink for one of the morphogens while the other still satisfies zero flux. The model now selects only patterns that are internal to the domain, and exhibits a patterning sequence that is consistent with that observed in the limb. The insight gained here then, is that the boundary plays an active role in the patterning mechanism, rather than simply being a passive impermeable membrane.

In 1990, Wolpert and Hornbruch performed an experiment in an attempt to prove that limb development in chick could not possibly arise as a consequence of a RD or mechanical mechanism of the sort discussed in this chapter. They removed the posterior half of a host limb bud and replaced it by the anterior half of a donor limb bud so that the resultant double-anterior recombinant limb bud was the same size as a normal limb bud. This experiment was performed at a sufficiently early stage in development that no pattern was visible. The limbs developed two humeri instead of one. This contradicted both models, due to the fact that the model solutions are size-dependent, that is, if the domain size is unaltered, the patterns produced are unaltered.

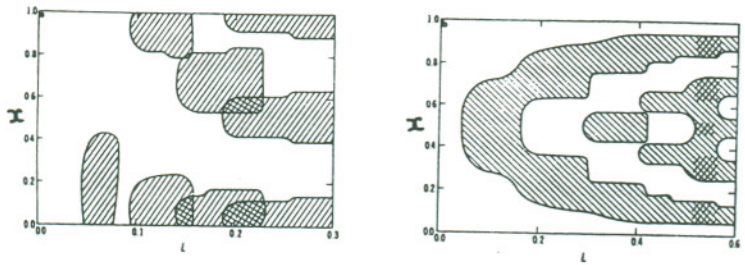

Figure 4.1: Subintervals of $(0,1)$ in which the v component of a typical RD system exceeds a fixed threshold as a function of length scale, L, for the cases (a) Neumann

boundary conditions on both species, (b) Neumann boundary conditions for u, homogeneous Dirichlet boundary conditions for v. (See Dillon *et al.*, 1994, for full details). Reproduced from Dillon *et al.*, 1994, by permission of Springer-Verlag.

However, this result is consistent with the theory if the model is modified. The nondimensionalisation in Section 1.2 shows that diffusion and length scale are intimately linked. Therefore, if we assume that the diffusion coefficient of the morphogen varies appropriately across the domain, this essentially sets up an internal scaling, where the length scale in one part of the domain can be made sufficiently small that it cannot support Turing structures. Therefore, although combining two anterior halves results in a limb bud of normal size, it might actually consist of doubling the patterning sub-domain and hence result in more complicated patterns. The prediction of the modelling was that there must be a variation of diffusion across the anterior-posterior axis of the chick limb (see Fig. 4.2 and Maini *et al.*, 1992). This actually agrees with experimental results which show that gap junction permeability varies across the anterior-posterior axis of the chick limb (see, for example, Brümmer *et al.*, 1991).

The above results are all for a one-dimensional domain. Recently, we have shown that the crucial patterning selection properties of different types of boundary conditions and internal scaling by spatially varying diffusion coefficients can be carried over to two-dimensional domains, producing patterns consistent with those observed in the limb (Myerscough *et al.*, 1997).

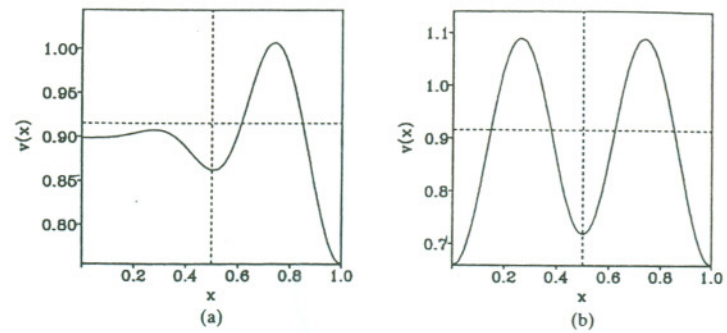

Figure 4.2: (a) Steady state solution for $v(x)$ to the Schnakenberg RD model with a spatially-varying diffusion coefficient of the form $D(x) = c_0 cosh\delta x / cosh\delta$. (b) Solution for the case where the $D(x)$ is symmetrical about $x = 1/2$ but identical to the case (a) on $(1/2, 1]$. For a suitable choice of threshold concentration (- - -) the prepattern in (a) specifies a single structure whereas that in (b) specifies two

structures even though the domain size has remained unchanged. (See Maini *et al.*, 1992, for full details). Reproduced from Maini *et al.*, 1992, by permission of Oxford University Press.

4.3 Pigmentation patterns in reptiles

The steady-state patterns exhibited by the cell-chemotactic (CC) model presented in Section 2 have been extensively studied in two dimensions and shown to be consistent with many characteristic skin pigmentation patterns on snakes (Maini *et al.*, 1991, Murray and Myerscough, 1991). However, here we focus on a different type of patterning, namely propagating patterns, with particular application to the pigmentation patterns of brown/black and white stripes on hatchling alligators. The white stripes are due to an absence of melanocytes (Murray *et al.*, 1990) and therefore it appears that a cell movement model in which high cell density results in pigmented regions while low cell densities lead to an absence of pigmentation, is a more realistic model than one based on reaction-diffusion. The pattern is initiated from the head and propagates down the head-tail axis. Murray *et al.*, (1990) showed that a CC model of the form illustrated in Section 2 can produce such propagating pattern (see Fig. 4.3). Note that the sharpness of the peaks is characteristic of CC models.

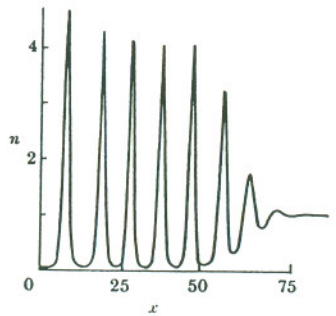

Figure 4.3: Propagating patterns exhibited by the CC model of Section 2 (Murray *et al.*, 1990). Reproduced from Murray *et al.*, 1990, by permission of The Royal Society, London.

4.4 Skin Organ Formation

During morphogenesis regular patterns often develop behind a frontier of pattern formation which travels across the prospective tissue. A simple example of such patterning was considered in Section 4.3. More complicated patterns can arise in,

for example, the structure of feather primordia. A feather primordium consists of a thickening (placode) of the epidermis overlying an aggregation of cells (papilla) in the dermis. The primordium initiates the formation of a feather. On the dorsal surface of the chick, feather primordia form in a specific sequence. Firstly, a row of primordia form along the dorsal midline. Subsequent rows form lateral to this initial row with the primordia in each row roughly 180° out of phase with those in the previous row, so that a rhombic pattern appears. This patterning process requires the interaction of both epidermis and dermis.

Perelson *et al.*, (1986) considered a version of the mechanical model of Section 3 and showed that it could give rise to sequential patterning in the dermis consistent with that observed experimentally. Once the initial row of pattern is set up due, for example, to the uniform steady state going unstable, it, in turn, sets up a strain field that causes cell aggregations in the adjacent rows to be situated 180° out of phase with those of the dorsal midline.

A more biologically realistic model was proposed by Cruywagen and Murray (1992) which includes tissue-tissue interaction. This model encorporates many of the key features of the models discussed in Sections 2 and 3 by coupling chemical interaction with mechanical effects in a mechanochemical model. Briefly, dermal cells secrete a chemical which diffuses into the epidermis where it stimulates cell traction. Epidermal cells secrete a chemical which diffuses into the dermis where it acts as a chemoattractant. Cruywagen *et al.*, 1992, show that tissue-tissue interaction is essential for this model to produce pattern and that the form of the full two-dimensional pattern is determined by the pattern along the dorsal midline. In other words, the specification of a simple quasi-one-dimensional pattern is all that is required to determine a complex two-dimensional pattern (see Fig. 4.4).

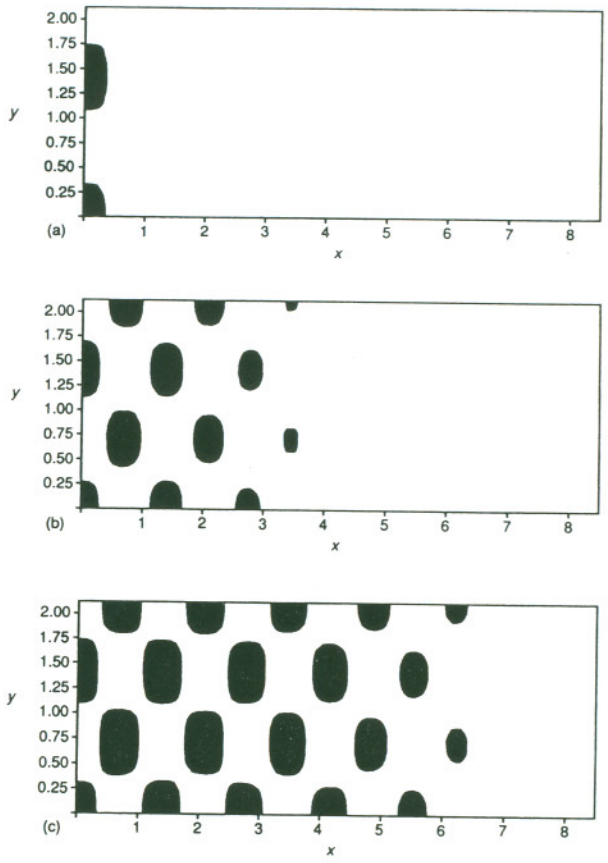

Figure 4.4: Sequential pattern formation in a tissue-tissue interaction mechanochemical model. Regions of high cell density are shaded. (a) Initially, a single row of spots of high cell density is specified at one end of a rectangular domain. As the system evolves, more rows are added sequentially as the pattern propagates across the domain; (b) and (c) show density profiles at subsequent times. (For full details, see Cruywagen *et al.*, 1992). Reproduced from Cruywagen *et al.*, 1992, by permission of Oxford University Press.

4.5 Coupled Pattern Generators

In Section 4.4 we considered a coupled mechanical-chemotaxis system. This model coupled the mechanical properties of the epidermis, with the chemotactic properties of dermal cells. Each tissue on its own was unable to produce patterns. The coupling was crucial to pattern formation: the dermal-epidermal interaction triggered "activation" in the epidermis by initiating cell traction; the epidermal-dermal interaction triggered "activation" in the dermis through chemotaxis. Here we briefly consider a coupled RD-CC model in which each model on its own can produce pattern. In this case the coupling enhances the complexity of the patterns formed (Painter *et al.*, in prep.).

Suppose that a cell population responds to two chemicals which themselves form a RD system. A possible model for this situation is the following:

$$\frac{\partial n}{\partial t} = D_n \nabla^2 n - \nabla.\{n\chi_u(u,v)\nabla u + n\chi_v(u,v)\nabla v\} \tag{4.1a}$$

$$\frac{\partial u}{\partial t} = D_1 \nabla^2 u + f(u,v,n) \tag{4.1b}$$

$$\frac{\partial v}{\partial t} = D_2 \nabla^2 v + g(u,v,n) \tag{4.1c}$$

where n, u and v are cell density and chemical concentrations, respectively, D_n, D_1, D_2 are diffusion coefficients and χ_u, χ_v are cell chemotactic responses to gradients in u and v, respectively.

For simplicity, let us assume that f and g do not depend on n, and that the time scale for the chemical dynamics is much faster than that of the cell dynamics. Then, in the appropriate parameter space, u and v will evolve to spatially-varying steady state patterns. If we restrict our attention for the moment to the one-dimensional domain $x \in [0,1]$, the steady state equation for n is

$$0 = D_n \frac{d^2 n}{dx^2} - \frac{d}{dx}\left(n\chi_u(u,v)\frac{du}{dx} + n\chi_v(u,v)\frac{dv}{dx}\right) \tag{4.2}$$

where u and v are at their steady states. Imposing zero flux boundary conditions, this equation can be integrated twice to give

$$n(x) = k \exp\left(\frac{1}{D_n}\int_0^1 \left(\chi_u \frac{du}{dx} + \chi_v \frac{dv}{dx}\right) dx\right) \tag{4.3}$$

where k can be evaluated using conservation of cell density.

One way to measure complexity of pattern is to calculate the number of turning points for a particular pattern. Critical points for $n(x)$ are given by

$$\chi_u \frac{du}{dx} + \chi_v \frac{dv}{dx} = 0. \tag{4.4}$$

For the parameter regimes wherein the subsystem (4.1b)-(4.1c) is close to a primary bifurcation point, we can use nonlinear analysis (Section 1.5) to derive analytic approximations for u and v. We can then substitute these expressions into (4.4) and, for the different chemotactic sensitivities described in Section 2, find if (4.4) has more solutions (corresponding to more complex pattern) than the number of critical points for the chemical concentrations. In this way, we can precisely measure how the complexity of pattern is enhanced by different modes of coupling.

The above analysis applies only to a one-dimensional domain and in the vicinity of a primary bifurcation point. A more extensive investigation of the solution properties of this model can be carried out using numerical simulations. Fig. 4.5 illustrates some typical patterns. Fig. 4.5a shows a one-dimensional pattern corresponding to thick and thin stripes. This kind of pattern can be generated by a pure CC model (Maini *et al.*, 1991). However, the pattern in Figure 4.5b cannot, to our knowledge, be exhibited by a simple pattern generator. Note that this pattern captures the intricate features of some animal coat markings, such as those on the jaguar.

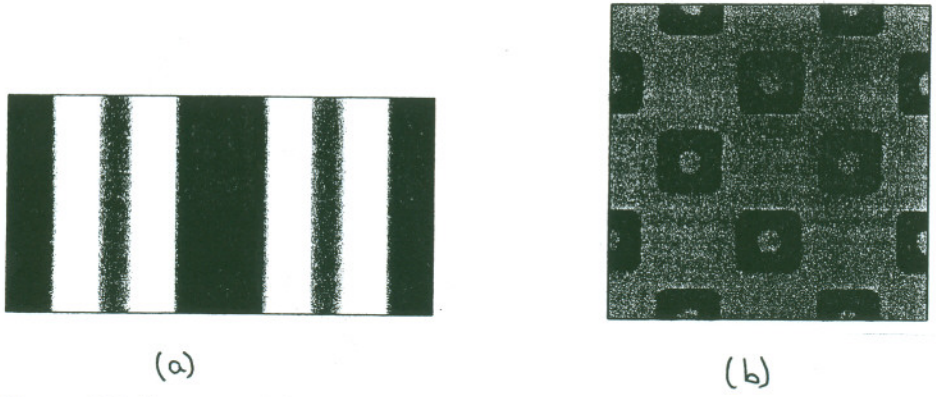

Figure 4.5: Patterns exhibited by coupling pattern generators. (a) A one-dimensional pattern in cell density corresponding to thick and thin stripes. (b) A two-dimensional pattern in which the intensity of shading represents cell density.

5 Conclusions

The study of coupled systems of reaction-diffusion equations was inspired by a mathematician wishing to understand the mechanisms underlying biological pattern formation. This led to the prediction that interacting chemicals could, under special conditions, lead to patterns in chemical concentrations. It has only recently been discovered that this is indeed the case and many patterns predicted by Turing type models have now been found experimentally (see Maini *et al.*, 1997, for a review of recent experimental results on spatial pattern formation in chemistry).

Since Turing's seminal paper, a number of other mechanisms have been proposed as pattern generators, most notable being the chemotactic and mechanical models described in this chapter. As mentioned in Section 4.1, many features of the patterns exhibited by these models are generic. This has the advantage of allowing one to make some general preditions irrespective of the detailed biology, but has the disadvantage of not allowing us to distinguish between biological mechanisms. There are some exceptions to this. For example, as discussed in Section 4.3, cell movement seems to play a key role in reptile pigmentation patterns suggesting that RD models are probably not appropriate. However, in such circumstances, a study of the simplest and most mathematically tractable model can still yield valuable insight due to the mechanism-independent mathematical properties of many of the patterns.

Acknowledgement: I would like to thank Brenda Willoughby for typing this manuscript.

References

J. Bard, A model for generating aspects of zebra and other mammalian coat patterns, *J. theor. Biol.*, **93**, 363-385 (1981)

J. Bard and I. Lauder, How well does Turing's theory of morphogenesis work? *J. theor. Biol.*, **45**, 501–531 (1974)

D.L. Benson, J.A. Sherratt and P.K. Maini, Diffusion driven instability in an inhomogeneous domain, *Bull. Math. Biol.*, **55**, 365-384 (1993)

D.L. Benson, P.K. Maini and J.A. Sherratt, Unravelling the Turing bifurcation using spatially varying diffusion coefficients, *J. Math. Biol.*, (1998) (to appear)

N. F. Britton, *Reaction-Diffusion Equations and Their Applications to Biology*, Academic Press, London, 1986

F. Brümmer, G. Zempel, P. Buhle, J.-C. Stein and D. F. Hulser, Retinoic acid modulates gap junction permeability: A comparative study of dye spreading and ionic coupling in cultured cells, *Exp. Cell. Res.*, **196,** 158–163 (1991)

V. Castets, E. Dulos, J. Boissonade and P. De Kepper, Experimental evidence of a sustained Turing-type equilibrium chemical pattern, *Phys. Rev. Lett.*, **64**(3), 2953–2956 (1990)

S. Childress and J.K. Percus, Nonlinear aspects of chemotaxis, *Math. Biosciences,* **56,** 217-237 (1981)

G.C. Cruywagen, P.K. Maini and J.D. Murray, Sequential pattern formation in a model for skin morphogenesis, *IMA J.Math.Appl.Med. & Biol.*, **9,** 227-248 (1992)

G.C. Cruywagen and J.D. Murray, On a tissue interaction model for skin pattern formation, *J. Nonlinear Sci.*, **2,** 217-240 (1992)

G. Dee and J.S. Langer, Propagating pattern selection, *Phys. Rev. Letts.*, **50(6),** 383-386 (1983)

P. De Kepper, V. Castets, E. Dulos and J. Boissonade, Turing-type chemical patterns in the chlorite-iodide-malonic acid reaction, *Physica D,* **49,** 161–169 (1991)

R. Dillon, P.K. Maini and H.G. Othmer, Pattern formation in generalised Turing systems: I. Steady-state patterns in systems with mixed boundary conditions, *J. Math. Biol.*, **32,** 345-393 (1994)

E. Doedel, AUTO: Software for continuation and bifurcation problems in ordinary differential equations. *Technical Report, Cal. Tech.*, 1986

B. Ermentrout, Stripes or spots? Nonlinear effects in bifurcation of reaction-diffusion equations on the square, *Proc. Roy. Soc. Lond.*, **A434,** 413-417 (1991)

P. Fife, *Mathematical Aspects of Reacting and Diffusing Systems, Lect. Notes in Biomath.*, **28,** Springer-Verlag, Berlin, Heidelberg, New York, 1979.

R.M. Ford, and D.A. Lauffenburger, Analysis of chemotactic bacterial distributions in population migration assays using a mathematical model applicable to steep or shallow attractant gradients, *Bull. Math. Biol.*, **53,** 721–749 (1991)

A. Gierer and H. Meinhardt, A theory of biological pattern formation, *Kybernetik,* **12,** 30-39 (1972)

A. Goldbeter, *Biochemical Oscillations and Cellular Rhythms: The molecular bases of periodic and chaotic behaviour,* Cambridge University Press (1996)

P. Grindrod, *The Theory of Applications of Reaction-Diffusion Equations: Pattern and Waves,* Oxford University Press, 1996

P. Grindrod, J.D. Murray and S. Sinha, Steady-state spatial patterns in a cell-chemotaxis model, *IMA J. Appl. Math. Med. & Biol.*, **6,** 69-79 (1989)

B.R. Johnson and S.K. Scott, New approaches to chemical patterns, *Chem. Soc. Rev.*, 265-273 (1996)

E.F. Keller and L.A. Segel, Travelling bands of bacteria: a theoretical analysis, *J. theor. Biol.*, **30,** 235-248 (1971)

L. Landau and E. Lipshitz, *Theory of Elasticity,* 2nd edn., New York, Pergamon, 1970

I.R. Lapidus, and R. Schiller, A model for the chemotactic response of a bacterial population, *Biophys. J.*, **16,** 779–789 (1976)

I. Lengyel and I.R. Epstein, Modeling of Turing structures in the chlorite-iodide-malonic acid-starch reaction system, *Science,* **251,** 650-652 (1991)

P.K. Maini, D.L. Benson and J.A. Sherratt, Pattern formation in reaction diffusion models with spatially inhomogeneous diffusion coefficients, *IMA J.Math.Appl.Med. & Biol.* 9, 197-213 (1992)

P.K. Maini, M.R. Myerscough, K.H. Winters and J.D.Murray, Bifurcating spatially heterogeneous solutions in a chemotaxis model for biological pattern formation, *Bull. Math. Biol.*, **53,** 701–719 (1991)

P.K. Maini, K.J. Painter and H. Chau, Spatial pattern formation in chemical and biological systems, *Faraday Transactions,* **93,** 3601–3610 (1997)

P.K. Maini and M. Solursh, Cellular mechanisms of pattern formation in the developing limb, *Int. Rev. Cytology,* 129, 91-133 (1991)

S.C. Müller, T. Plesser and B. Hess, The structure of the core of the spiral wave in the Belousov-Zhabotinskii reaction, *Science,* **230,** 661-663 (1985)

J.D. Murray, Parameter space for Turing instability in reaction diffusion mechanisms: a comparison of models, *J. theor. Biol.*, **98,** 143-163 (1982)

J.D. Murray, *Asymptotic Analysis,* 2nd edn., Berlin Heidelberg New York Tokyo, Springer (1984)

J.D. Murray, *Mathematical Biology,* 2nd edn., Berlin, Heidelberg, New York, London. Paris, Tokyo, Springer-Verlag (1993)

J.D. Murray, D.C. Deeming and M.W.J. Ferguson, Size dependent pigmentation pattern formation in embryos of Alligator mississippiensis: time of initiation of pattern generation mechanism, *Proc. Roy. Soc. Lond.*, **B 239,** 279-293 (1990)

J.D. Murray and M.R. Myerscough, Pigmentation pattern formation on snakes, *J. theor. Biol.*, **149,** 339-360 (1991)

M.R. Myerscough, P.K. Maini and K.J. Painter, Pattern formation in a generalised chemotactic model, *Bull. Math., Biol.*, (1997) (to appear)

M.R. Myerscough and J.D. Murray, Analysis of propagating pattern in a chemotaxis system, *Bull. Math. Biol.*, **54,** 77-94 (1992)

G.A. Ngwa and P.K. Maini, Spatio-temporal patterns in a mechanical model for mesenchymal morphogenesis, *J. Math. Biol.*, 33, 489-520 (1995)

H.G. Othmer and A. Stevens, Aggregation, Blow-up and Collapse: The ABCs of taxis inreinforced random walks, *SIAM J.Appl.Math* (to appear)

Q. Ouyang, R. Li, G. Li and H.L. Swinney, Dependence of Turing pattern wavelength on diffusion rate, *J. Chem. Phys.*, **102**(6), 2551-2555 (1995)

G.F. Oster, J.D. Murray and A.K. Harris, Mechanical aspects of mesenchymal morphogenesis, *J. Embryol.exp. Morph.*, **78,** 83-125 (1983)

G.F. Oster, N. Shubin, J.D. Murray and P. Alberch, Evolution and morphogenetic rules. The shape of the vertebrate limb in ontogeny and phylogeny, *Evolution,* **45,** 862-884 (1988)

K.J. Painter, P.K. Maini and H.G. Othmer, Spatial pattern formation in coupled cell-chemotactic-reaction-diffusion systems (in prep.)

A.V. Panfilov and A.V. Holden (eds), *Computational Biology of the Heart,* John Wiley & Sons (1997)

A.S. Perelson, P.K. Maini, J.D. Murray, J.M. Hyman and G.F. Oster, Nonlinear pattern selection in a mechanical model for morphogenesis, *J. Math. Biol.*, 24, 525-541 (1986)

D.H. Sattinger, Six lectures on the transition to instability, in *Lecture Notes in Mathematics*, **322**, Berlin, Springer-Verlag (1972)

J. Schnakenberg, Simple chemical reaction systems with limit cycle behaviour, *J. theor. Biol.*, **81,** 389-400 (1979)

D. Thomas, Artifical enzyme membranes, transport, memory and oscillatory phenomena, in *Analysis and Control of Immobilized Enzyme Systems*, ed. D. Thomas and J.-P. Kernevez, Springer, Berlin, Heidelberg, New York, 115-150 (1975)

A. M. Turing, The chemical basis of morphogenesis, *Phil. Trans. Roy. Soc. Lond,* **B327,** 37-72 (1952)

B.J. Welsh, J. Gomatam and A.E. Burgess, Three-dimensional chemical waves in the Belousov-Zhabotinskii reaction, *Nature,* **340,** 611-614 (1983)

A.T. Winfree, Spiral waves of chemical activity, *Science,* **175,** 634-636 (1972)

A.T. Winfree, Rotating chemical reactions, *Sci. Amer.*, **230**(6), 82-95 (1974)

L. Wolpert, Positional information and the spatial pattern of cellular differentiation, *J. theor. Biol.*, **25,** 1-47 (1969)

L. Wolpert and A. Hornbruch, Double anterior chick limb buds and models for cartilage rudiment specification, *Development,* **109,** 961-966 (1990)

A.N. Zaikin and A.M. Zhabotinskii, Concentration wave propagation in two-dimensional liquid-phase self-organising system, *Nature,* **225,** 535-537 (1970)

V.S. Zykov, *Simulation of Wave Processes in Excitable Media,* Manchester University Press (1987)